

# MAGNETIC FLUX CANCELLATION OBSERVED IN THE SUNSPOT MOAT

VASYL B. YURCHYSHYN<sup>1,2</sup> and HAIMIN WANG<sup>2</sup>

<sup>1</sup>*Big Bear Solar Observatory, Big Bear City, CA 92314, U.S.A. (e-mail: vayur@bbsso.njit.edu)*

<sup>2</sup>*Crimean Astrophysical Observatory, 98409, Nauchny, Crimea, Ukraine*

(Received 2 November 2000; accepted 22 May 2001)

**Abstract.** In this paper we study the evolution of magnetic fields of a 1F/2.4C solar flare and following magnetic flux cancellation. The data are Big Bear Solar Observatory and SOHO/MDI observations of active region NOAA 8375. The active region produced a multitude of subflares, many of them being clustered along the moat boundary in the area with mixed polarity magnetic fields. The study indicates a possible connection between the flare and the flux cancellation. The cancellation rate, defined from the data, was found to be  $3 \times 10^{19} \text{ Mx h}^{-1}$ . We observed strong upward directed plasma flows at the cancellation site. Suggesting that the cancellation is a result of reconnection process, we also found a reconnection rate of  $0.5 \text{ km s}^{-1}$ , which is a significant fraction of Alfvén speed. The reconnection rate indicates a regime of fast photospheric reconnection happening during the cancellation.

## 1. Introduction

The occurrence of solar flares is believed to be related to the presence of various irregularities in the magnetic field structure caused by photospheric activity. These include particular values of the magnetic fields, sheared sunspot motions (Hagyard *et al.*, 1984), new magnetic flux emergence (Heyvaerts, Priest, and Rust, 1977), specific magnetic field patterns such as an S-shaped neutral line (Gorbachev and Somov, 1988) or close proximity of different magnetic polarities (Martin, Livi, and Wang, 1985). A necessary condition for a solar flare to occur is the rearrangement of the photospheric magnetic field caused by continuous shuffling and braiding motions of photospheric magnetic elements. This photospheric ‘diffusion’ process leads to magnetic flux cancellation at the polarity inversion line. Magnetic reconnection is believed to be the principal mechanism for extracting free energy from the magnetic field and converting it into plasma heating and mass ejection (Priest and Forbes, 1986). However, in spite of the fact that magnetic reconnection is invoked in many theories, our knowledge of the process derived from observational data is still mainly qualitative. Apart from the existence of fast reconnection in the corona, the possibility of rapid photospheric reconnection and its key role in many solar phenomena was not realized until recently (Roumeliotis and Moore, 1993; Litvinenko and Somov, 1994; Litvinenko, 1999).



Litvinenko (1999) derived parameters of the Sweet–Parker reconnection model in the photosphere. This model relates the cancellation rate and inflow velocity in a current sheet to the magnetic field strength and it has only been successfully tested in two cases: weak (quiet Sun) and strong (active region) fields. Application of the model to a large data set will prove its ability to properly describe photospheric reconnection. We need to analyze more cases in detail to establish the ways an active region may release its free energy and, what is more important, to derive reliable physical characteristics of the magnetic configuration. The identification of the relevant properties of the magnetic field is important for developing and testing theoretical models and for forecasting flare activity.

We focus here on a 1F/C2.4 flare out of many subflares which occurred in vicinity of a large sunspot and magnetic flux cancellation following the flare. The data consist of an uninterrupted time series of white-light, magnetic field and H $\alpha$  observations (Section 2). Precise tracking of magnetic features prior to and after the flare enabled us to understand the evolution of the magnetic fields and to derive physical parameters of the evolving system (Section 3). We present a short summary in Section 4.

## 2. Data

The data consist of BBSO and SOHO/MDI observations of a large rapidly evolving sunspot with an extended plage region (Figure 1). The active region NOAA AR 8375 appeared on the solar disk as a single sunspot on 28 October 1998 and produced a multitude of subflares, many of them being clustered along the moat boundary with a distinctive magnetic character (for more details see also Wang *et al.*, 2000; Yurchyshyn *et al.*, 2000; Yurchyshyn, Wang, and Goode, 2001). Uninterrupted SOHO/MDI observations continued for three successive days (3–6 November 1998) with a time cadence of 1 min.

The BBSO observations completely covered the passage of the active region across the solar disk. High-resolution H $\alpha$  images were obtained by the 65-cm reflector with a time cadence of 30 s and a pixel size 0.3". Line-of-sight videomagnetograms were obtained with the 25-cm refractor. The pixel resolution was 0.6", and the time cadence was 30 s.

The BBSO videomagnetograms and H $\alpha$  images were accurately re-scaled and coaligned (coalignment accuracy was better than 1") with SOHO/MDI intensity images using plage and sunspot positions. The field of view of all the images is 219"  $\times$  163" at a scale of 0.625" per pixel.

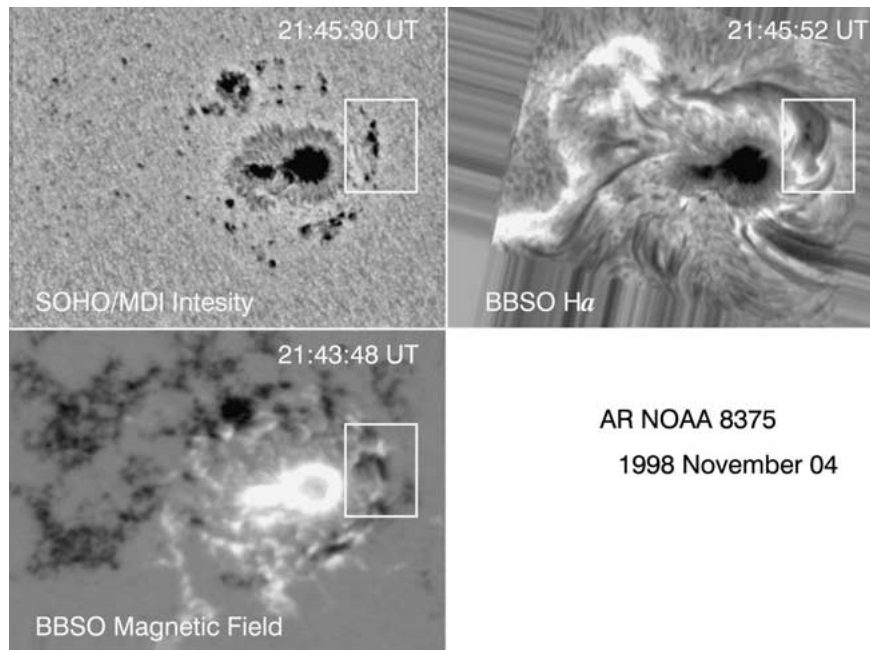


Figure 1. BBSO and SOHO/MDI observations of AR 8375. The box shows the area where photospheric flux cancellation was observed.

### 3. Proper Motions of Magnetic Elements and Flux Cancellation

According to the GOES X-ray flux measurements, on 4 November 1998 a 1F/2.4C flare started at 22:02 UT and lasted for 12 min. Figure 2 shows the BBSO  $H\alpha$  images of the flare and the corresponding longitudinal magnetic field. In the figure, dashed curves mark a pre-existing  $H\alpha$  loop, L1, which disappeared during the course of the flare. After the flare onset, at 22:07:22 UT, we could distinguish two loops: the pre-existing loop, L1, and a newly formed loop, L2, which share the same magnetic polarity at the closer-spaced footpoints. As the flare proceeds, the large-scale bright loop L2 rises into the corona and gradually fades. The growth velocity of the top of the loop increased from approximately 60 up to 110  $\text{km s}^{-1}$  over 3 min. In the videomagnetogram recorded at 21:59:08 UT we show the location of the  $H\alpha$  loops in respect to the magnetic field. From the figure one can see that the loop L1 has one footpoint rooted near the leading sunspot, while the second one is located in the small magnetic element of S polarity (marked with P1 in Figure 2). The P1 magnetic element had a neighbor – a magnetic island of N polarity, P2.

Figure 3 shows the 19-hour time series of SOHO/MDI intensity images, which are the enlarged area indicated by rectangle in Figure 1. In the image taken at 03:00:30 UT the pores were well separated at a distance of about 13000 km. We marked starting positions of the pores with short dashed lines. Current positions

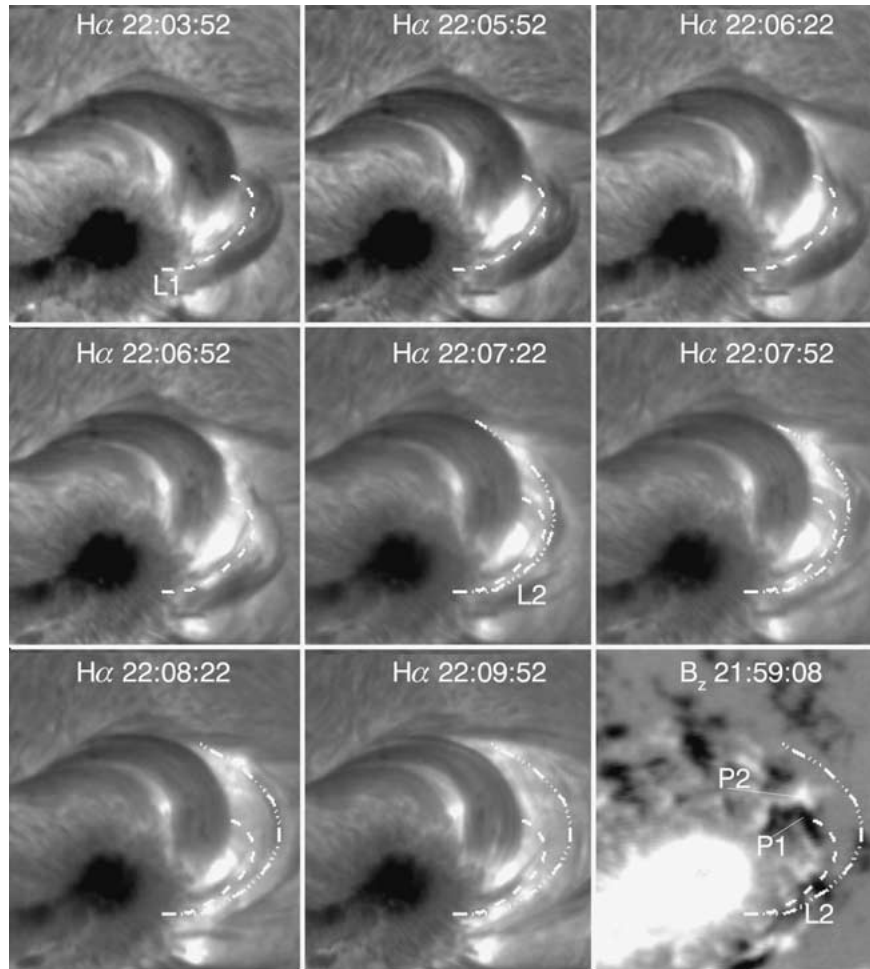


Figure 2. BBSO observations of the flare development. *Dashed curve* marks a pre-existing H $\alpha$  loop, L1, which disappeared during the course of the flare. *Dash-dotted lines* shows a newly formed loop, L2. In the videomagnetogram (*bottom right image*) we show the location of the H $\alpha$  loops in respect to the magnetic field.

of the pores are shown with solid lines. At 03:00:30 UT, the approach speed of the pores was about  $250 \text{ m s}^{-1}$ . Before the encounter, both pores slowed down to  $70 \text{ m s}^{-1}$  (see also Martin, 1985). The pores then slightly increased in size and, by 21:00:30 UT, they created clusters of pores of a variety of sizes. By this time, they were separated by about 4500 km. The maximum field strengths in the approaching magnetic elements was found to be about 650 G, which implies a horizontal gradient of the longitudinal magnetic field before the flare of  $0.29 \text{ G km}^{-1}$ .

Figure 4 shows a further stage of the evolution. There are six pairs of images. Each pair consists of BBSO videomagnetograms (top row) and SOHO/MDI intensity images (bottom row), both taken at the same time. The P2 pore disappears in

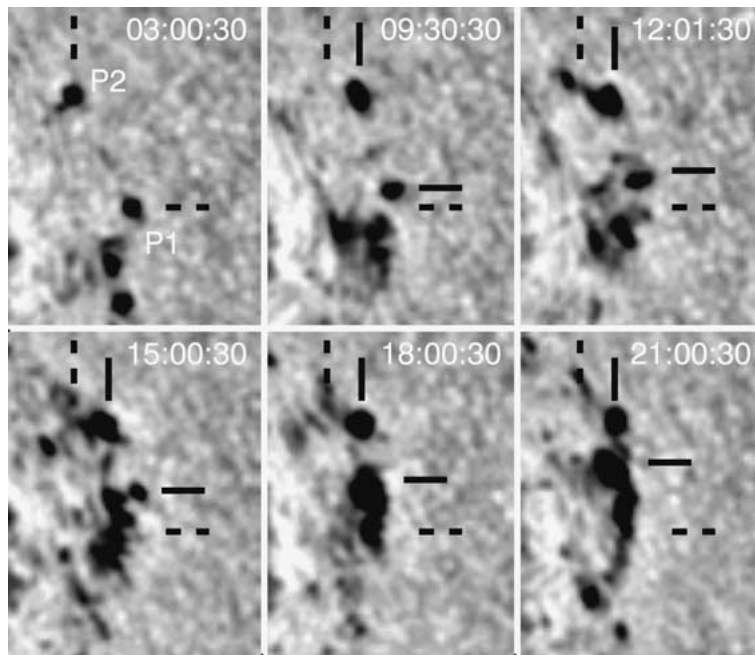


Figure 3. SOHO/MDI intensity images showing the moving magnetic pores P1 and P2. Dashed lines show the position of the pores at 03:00 UT. Solid lines mark the current position of the pores.

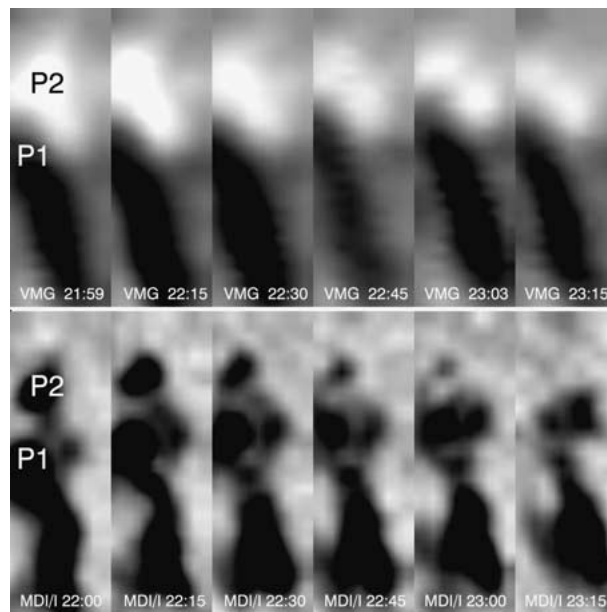


Figure 4. Top row: BBSO magnetic field measurements at the cancellation site. Black (white) shows the magnetic field greater than 400 G. Bottom row: the SOHO/MDI intensity distribution at the cancellation site. One sees complete disappearance of the P2 pore.

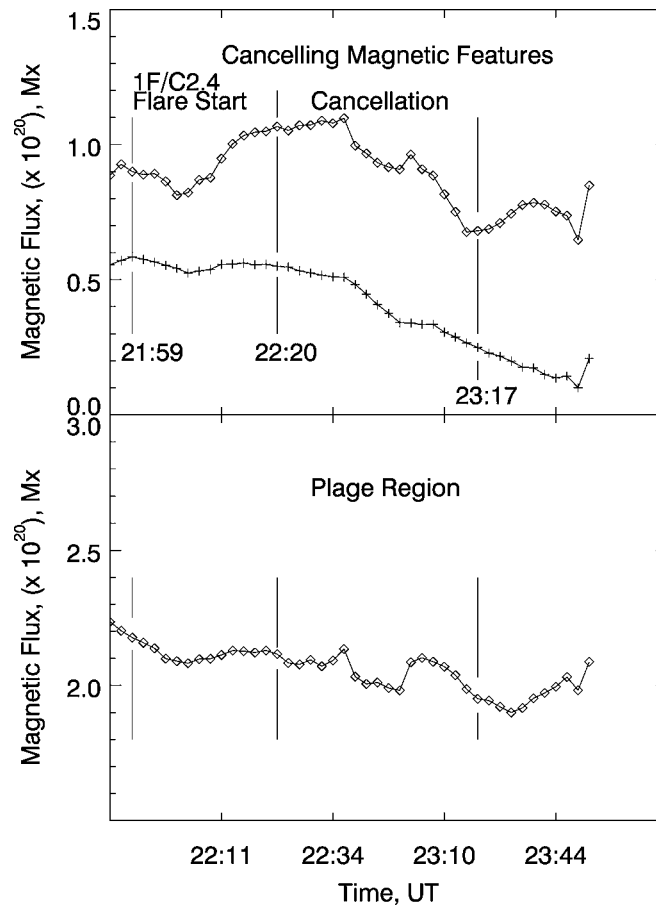


Figure 5. Magnetic flux changes at the cancellation site (*top plot*) and at a plage region east of the sunspot. *Pluses (diamonds)* show the positive (negative) magnetic flux. The scales of the vertical axes are the same in both plots.

the MDI images while in the BBSO magnetograms the magnetic fragments have decreased in size and the magnetic field strength lowered from 650 G to 350 G. By 23:15 UT, the P2 pore had completely disappeared from the field of view and only a dark intergranular lane was left at that place. Thus, we observed the magnetic flux cancellation happening after a solar flare, where equal amounts of magnetic flux should disappear.

We calculated a total positive and a total negative magnetic flux through the area shown in Figure 4 (cancelling magnetic features). To obtain a reliable result, we used 50 longitudinal magnetograms recorded prior to and after the flare. Figure 5 shows the result. The top plot shows the variation of magnetic flux in the cancelling magnetic features. The first two vertical lines mark the beginning of the flare and the end. The third vertical marks the end of the cancellation. During the flare, one cannot see any noticeable signs of magnetic cancellation. The flux started to

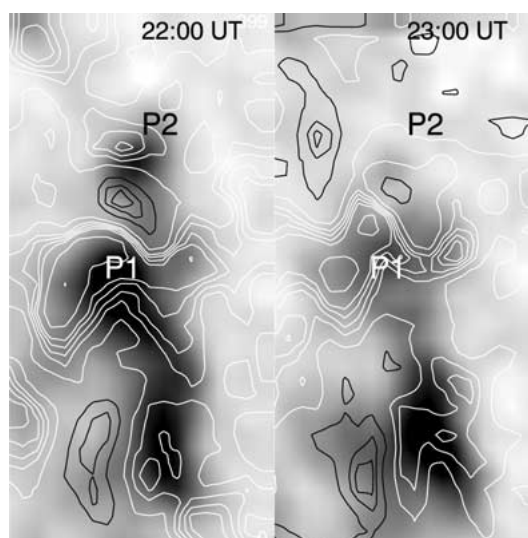


Figure 6. Gray-scale image showing the MDI intensity in the two pores P1 and P2. Contours represent the MDI Doppler velocity field (black contours – upflow) and refer to velocities of 200, 400, 500  $\text{m s}^{-1}$ .

decrease at about 22:34 UT, 14 min after the end of the flare. To eliminate the flux variations due to seeing we also calculated magnetic flux through an area which includes the plage magnetic field far away in the trailing part of the active region. One sees that the magnetic flux gradually decreased in both pores by  $4 \times 10^{19}$  Mx during the corresponding cancellation time  $t = 1$  h (top plot). During the same time in the plage region, the magnetic flux decreased by only  $1 \times 10^{19}$  Mx (bottom plot), which implies a cancelled magnetic flux of  $\Phi = 3 \times 10^{19}$  Mx and a cancellation rate  $R = 3 \times 10^{19}$  Mx  $\text{h}^{-1}$ . This is two orders of magnitude higher than that obtained by Harvey (1985) in quiet-Sun features and corresponds to the cancellation rate inferred by Litvinenko and Martin (1999).

Martin (1990, see also Priest, Parnell, and Martin, 1994) suggested that observed photospheric flux cancellation is due to a reconnection process in the photosphere rather than simple submergence of the magnetic field. Although it is nearly impossible to observe submergence of the reconnected loops, Harvey *et al.* (1999) presented observations proving that the reconnected loops shrink down and submerge under the solar surface with the vertical speed being in range  $0.3\text{--}1.0$  km  $\text{s}^{-1}$ . While magnetic reconnection is a common process in the corona and the rate of magnetic reconnection has been extensively studied (Dere, 1996), there are only a few reliable estimations of the rate of photospheric reconnection (Roumeliotis and Moore, 1993; Litvinenko and Martin, 1999).

There is a reason to speculate that the reconnection site was located at the photospheric level. It was shown that strong plasma jets from the current sheet are part of reconnection of noncollinear flux tubes (Furusawa and Sakai, 2000).

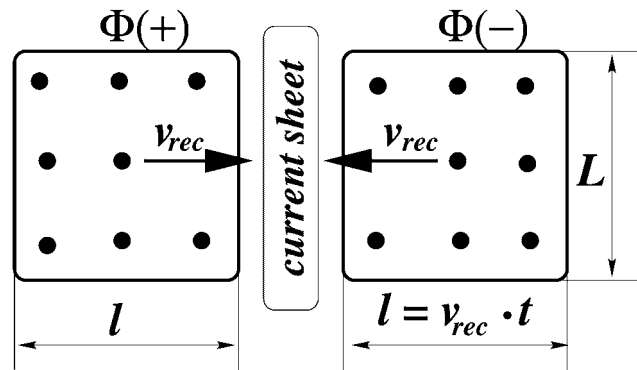


Figure 7. Schematic representation of reconnection process. Two magnetic fluxes  $\Phi(+)$  and  $\Phi(-)$  reconnect over time  $t$ .

In this case one should observe motions of the newly formed loops and upward jets above the reconnection site. Figure 6 shows the Doppler velocity field at the cancellation site. During the flare an upflow with a maximum velocity of  $600 \text{ m s}^{-1}$  was observed between the pores. The presence of the upflow indicates that the level of the Ni 6767 Å line formation (200 km above  $\tau_{5000}$  level, Jones, 1989) was located at, or above the reconnection site, which in turn places the reconnection site at the photospheric level. Note that according to the Sweet–Parker model, the outflow should proceed at the Alfvén speed in the photosphere, which does not exceed several kilometers per second.

To estimate the reconnection rate, we consider a simplified rectangular cross-section of two magnetic loops (Figure 7). We assume that the fields, each of strength  $B'$ , are in contact over a length  $L$  and merge with a velocity (reconnection rate)  $v_{\text{rec}}$  and reconnect. The area of the cross-section can be calculated as  $A = lL = Lv_{\text{rec}}t$  and the magnetic flux through the area is  $\Phi = AB'$ . This gives us the reconnection rate  $v_{\text{rec}}$  as follows:

$$v_{\text{rec}} = \frac{\Phi}{B'Lt}. \quad (1)$$

On the other hand, according to Litvinenko and Martin (1999) the reconnection rate  $v_{\text{rec}}$  is determined by the cancellation rate  $R$ :

$$v_{\text{rec}} = \frac{R}{BL}, \quad (2)$$

where  $B$  is the magnetic field strength,  $L$  is the length of the current sheet and  $R$  is the cancellation rate. As we see, both equations become identical when we replace  $R$  by  $\Phi/t$ .

All parameters but the field strength  $B'$  can be measured directly from the observations:  $\Phi/t = R = 3 \times 10^{19} \text{ Mx h}^{-1}$  and  $L = 3 \times 10^8 \text{ cm}$  (measured as the length of the neutral line between the pores P1 and P2). The reconnection

rate is partially defined by the local field  $B'$  in the vicinity of the current sheet, which cannot be measured directly. However, because the reconnection site was located very close to the level where the fields were measured and because of a possible pile-up of magnetic field at the current sheet (Priest and Forbes, 1986), we expect that the field  $B'$  is not much lower than the maximum photospheric field  $B \sim 650$  G in the cancelling elements. Substituting our direct measurements into Equation (2) produces the reconnection rate  $v_{\text{rec}} = 0.5 \text{ km s}^{-1}$ . The derived value of the reconnection rate is much larger than the approach speed of cancelling magnetic features. One source of uncertainty is the magnetic field strength in the vicinity of the current sheet, which we could overestimate by at most a factor of 2. Other possible sources, which could contribute to the discrepancy, have been pointed out by the referee. They include a larger than observed averaged speed of the cancelling features and/or the possibility that reconnection is responsible only for some fraction of the cancelled flux.

In general, the rate of reconnection is determined principally by the Alfvén speed  $V_A$  causing the reconnection generally to proceed with a speed  $v_{\text{rec}} = V_A/n$ , where  $n$  might be as small as unity and as large as  $10^3$  (Parker, 1972; Dere, 1996, and references therein). Assuming an Alfvén speed in the photosphere of several kilometers per second, a reconnection rate of  $v_{\text{rec}} \approx V_A/10$  is a significant fraction of the Alfvén speed and this places the rate of the magnetic reconnection in the regime of fast reconnection.

As we established earlier, the cancelled magnetic element P1 was identified as a footpoint of the chromospheric loop L1 (Figure 2), which in turn was part of the flare. This fact may imply that there is a connection between the flare and the cancellation. If so, the flare may be interpreted in the frame of the converging flux model (Priest, Parnell, and Martin, 1994), where photospheric flows push together two magnetic fragments and photospheric reconnection is most likely to proceed in a flux pile-up regime (Priest and Forbes, 1986). According to the model, the newly formed loops are ejected upward in the corona (see Figure 2, loop L2) and downward below the solar surface (flux cancellation). The model also indicates that after the rapid increase, the height of the reconnection point decreases toward zero as the fragments approach each other. If we interpret the time delay between the flare start and the cancellation (about 30 min) as time needed for magnetic loops to submerge from the height of about 200 km under the photosphere, then the speed of the submergence is about  $0.1 \text{ km s}^{-1}$ , which is consistent with results by Harvey *et al.* (1999).

#### 4. Summary

In summary, we have studied photospheric magnetic flux cancellation preceded by a 1F/C2.4 flare. The study shows that one footpoint of the chromospheric magnetic loop involved in the flare was rooted in the cancelled magnetic element, which

indicates a possible connection between the flux cancellation and the flare. The cancellation proceeded at a cancellation rate of  $3 \times 10^{19} \text{ Mx h}^{-1}$ . The reconnection rate,  $v_{\text{rec}} = 0.5 \text{ km s}^{-1}$ , defined from the observations, is a significant fraction of Alfvén speed, which indicates the regime of fast photospheric reconnection.

### Acknowledgements

We are grateful to an unknown referee for critical comments and valuable suggestions that improved the manuscript. We also thank P. Gallagher for careful reading and critical comments on the manuscript. This work was supported in part by NSF-ATM (97-14796) and NASA (NAG5-9682) grants. SOHO is a project of international cooperation between ESA and NASA.

### References

- Dere, K. P.: 1996, *Astrophys. J.* **472**, 864.  
 Furusawa, K. and Sakai, J.-I.: 2000, *Astrophys. J.* **540**, 1156.  
 Gorbachev, V. S. and Somov, B. V.: 1988, *Solar Phys.* **117**, 77. Hagyard, M. J., Smith, J. B., Jr., Teuber, D., and West, E. A.: 1984, *Solar Phys.* **91**, 115.  
 Harvey, K. L.: 1985, *Australian J. Phys.* **38**, 875.  
 Harvey, K. L., Jones, H. P., Schrijver, C. J., and Penn, M. J.: 1999, *Solar Phys.* **190**, 35.  
 Heyvaerts, J., Priest, E. R., and Rust, D. M.: 1977, *Astrophys. J.* **216**, 123.  
 Jones, H. P.: 1989, *Solar Phys.* **120**, 211.  
 Litvinenko, Y.: 1999, *Astrophys. J.* **515**, 435.  
 Litvinenko, Y. and Martin, S. F.: 1999, *Solar Phys.* **190**, 45.  
 Litvinenko, Y. and Somov, B. V.: 1994, *Solar Phys.* **151**, 265.  
 Martin, S.: 1988, *Solar Phys.* **117**, 243.  
 Martin, S.: 1990, in J.O. Stenflo (ed), *Solar Photosphere: Structure, Convection, and Magnetic Fields*, Kluwer Academic Publishers, Dordrecht, Holland, p. 129.  
 Martin, S. F., Livi, S. H. B., and Wang, J.: 1985, *Austr. J. Phys.* **38**, 929.  
 Parker, E. N.: 1972, *Astrophys. J.* **174**, 499.  
 Priest, E. R. and Forbes, T. G.: 1986, *J. Geophys. Res.* **91**, 5579.  
 Priest, E. R., Parnell, C. E., and Martin, S. F.: 1984, *Astrophys. J.* **427**, 459.  
 Roumeliotis, G. and Moore, R. L.: 1993, *Astrophys. J.* **416**, 386.  
 Wang, H., Goode, P. R., Denker, C., Yang, G., Yurchyshyn, V., Nitta, N., Gurman, J. B., Cyr, C. St., and Kosovichev, A. G.: 2000, *Astrophys. J.* **536**, 971.  
 Yurchyshyn, V. B., Wang, H., and Goode, P. R.: 2001, *Astrophys. J.*, **550**, 470.  
 Yurchyshyn, V. B., Wang, H., Qiu, J., Goode, P. R., and Abramenko, V. I.: 2000, *Astrophys. J.* **540**, 1143.